Developmental Biology 439 (2018) 53–64

Contents lists available at ScienceDirect

Developmental Biology

journal homepage: www.elsevier.com/locate/developmentalbiology

Direct visualization of the Wntless-induced redistribution of WNT1 in developing chick embryos

Lisa M. Galli[a], Frederick Santana[a], Chantilly Apollon[b], Linda A. Szabo[a,1], Keri Ngo[a], Laura W. Burrus[a,*]

[a] Department of Biology, San Francisco State University, 1600 Holloway Avenue, San Francisco, CA 94132, USA
[b] Department of Biology, Holy Names University, 3500 Mountain Boulevard, Oakland, CA 94619, USA

ARTICLE INFO

Keywords:
Palmitoylation
Live imaging
WNT1
WNT3A
WNT7A
PORCN
WLS
Chick
Zebrafish
Neural crest
Ectoderm
Filopodia
eGFP
moxGFP
mCherry
Membrane trafficking

ABSTRACT

Paracrine Wnt signals are critical regulators of cell proliferation, specification, and differentiation during embryogenesis. Consistent with the discovery that Wnt ligands are post-translationally modified with palmitoleate (a 16 carbon mono-unsaturated fatty acid), our studies show that the vast majority of bioavailable chick WNT1 (cWNT1) produced in stably transfected L cells is cell-associated. Thus, it seems unlikely that the WNT1 signal is propagated by diffusion alone. Unfortunately, the production and transport of vertebrate Wnt proteins has been exceedingly difficult to study as few antibodies are able to detect endogenous Wnt proteins and fixation is known to disrupt the architecture of cells and tissues. Furthermore, vertebrate Wnts have been extraordinarily refractory to tagging. To help overcome these obstacles, we have generated a number of tools that permit the detection of WNT1 in palmitoylation assays and the visualization of chick and zebrafish WNT1 in live cells and tissues. Consistent with previous studies in fixed cells, live imaging of cells and tissues with overexpressed cWNT1-moxGFP shows predominant localization of the protein to a reticulated network that is likely to be the endoplasmic reticulum. As PORCN and WLS are important upstream regulators of Wnt gradient formation, we also undertook the generation of mCherry-tagged variants of both proteins. While co-expression of PORCN-mCherry had no discernible effect on the localization of WNT1-moxGFP, co-expression of WLS-mCherry caused a marked redistribution of WNT1-moxGFP to the cell surface and cellular projections in cultured cells as well as in neural crest and surface ectoderm cells in developing chick embryos. Our studies further establish that the levels of WLS, and not PORCN, are rate limiting with respect to WNT1 trafficking.

1. Introduction

During vertebrate development, a single morphogen, such as Wnt, can pattern an entire field of cells. This remarkable feat is accomplished by the formation of a morphogen gradient, which then elicits concentration-dependent effects in target cells. As Wnt proteins have signal peptides and are targeted to the secretory pathway, it was long assumed that they are secreted proteins, which travel to target cells via diffusion (Brown et al., 1987; Papkoff et al., 1987; Smolich et al., 1993). However, two observations have challenged this assumption. First, Wnts are poorly secreted from virtually all cell types. Second, Wnts are post-translationally modified with palmitoleate, a 16-carbon mono-unsaturated fatty acid (Takada et al., 2006; Willert et al., 2003). Because of the hydrophobic nature of this modification, it is unlikely that palmiteoylated Wnts are freely soluble and diffusible in an aqueous solution.

These observations led to the formulation of new diffusion-dependent and -independent models. For example, data showing that WNT3A expressed in stably transfected mouse L cells can be secreted in association with lipoprotein-like particles and with exosomes led to two new diffusion-dependent models in which Wnts associated with either lipoprotein-like particles or exosomes diffuse to target cells (Gross et al., 2012; Neumann et al., 2009). By contrast, diffusion-independent models have Wnts tethered to the plasma membrane. In the simplest case model, membrane-tethered Wnts signal adjacent cells. Evidence from the colon crypt suggests that the distribution of Wnts into gradients is achieved by cell division (Farin et al., 2016). A final diffusion-independent model proposes that Wnts travel to target cells via long signaling filopodia (Huang and Kornberg, 2015; Luz et al., 2014; Stanganello et al., 2015). While this model has gained much traction in invertebrate systems, only two other groups have been successful in tackling this in vertebrate embryos (Luz et al., 2014; Stanganello et al., 2015).

* Correspondence to: San Francisco State University, 1600 Holloway Avenue, San Francisco, CA 94132, USA.
E-mail address: LBurrus@sfsu.edu (L.W. Burrus).
[1] Current Address: Driver Genomics LLC, 1700 Owens Street #405, San Francisco, CA 94158, USA.

https://doi.org/10.1016/j.ydbio.2018.04.025
Received 2 February 2018; Received in revised form 26 April 2018; Accepted 26 April 2018
Available online 30 April 2018
0012-1606/

At least two technical issues have contributed to the difficulty of studying Wnt gradient formation in vertebrate tissues. First, signaling filopodia are typically sensitive to fixation (Ramirez-Weber and Kornberg, 1999). Thus, the direct visualization of Wnts must be achieved in living tissues. To do this, it is necessary to generate a fluorophore-tagged Wnt protein that retains biological activity. Unfortunately, vertebrate Wnts are incredibly refractory to tagging. To date, only two Wnts, XWnt2B and zebrafish Wnt8A, have been successfully tagged with GFP (Holzer et al., 2012; Luz et al., 2014; Stanganello et al., 2015). Secondly, overexpression of Wnt proteins typically leads to the accumulation of Wnt protein in the endoplasmic reticulum and Golgi, with little or no Wnt protein being detectable on the cell surface or in filopodia (Burrus and McMahon, 1995). Thus, we predicted that overexpression of an upstream regulator of Wnt trafficking and secretion might be needed to direct ectopic Wnt to the surface.

Previous studies have shown that Porcupine (PORCN) and Wntless (WLS) are critical regulators of Wnt trafficking/secretion (Bänziger et al., 2006; Bartscherer et al., 2006; Galli et al., 2016b; Goodman et al., 2006; Takada et al., 2006; van den Heuvel et al., 1993). While PORCN is the enzyme that catalyzes the addition of palmitate to Wnt proteins (Takada et al., 2006), WLS is a cargo transporter that carries palmiteoylated Wnt to the cell surface (Bänziger et al., 2006; Bartscherer et al., 2006; Coombs et al., 2010; Goodman et al., 2006; Herr and Basler, 2012). The importance of these two proteins is highlighted by the observation that PORCN or WLS deficient mice arrest at gastrulation (Barrott et al., 2011; Biechele et al., 2011; Fu et al., 2009). In the absence of either PORCN or WLS, Wnt proteins are retained in the endoplasmic reticulum and are not secreted (Bänziger et al., 2006; Barrott et al., 2011; Bartscherer et al., 2006; Goodman et al., 2006; Takada et al., 2006; van den Heuvel et al., 1993). An additional study shows that only very minute quantities of PORCN are needed for proper Wnt signaling (Proffitt and Virshup, 2012). Consistent with this report, our previous studies show that co-expression of WLS, but not PORCN, with WNT1 significantly enhances Wnt signaling (Galli et al., 2016b). Thus, we hypothesized that co-expression of WLS along with WNT1 would lead to a dramatic redistribution of WNT1 from the endoplasmic reticulum to the cell surface, and possibly filopodia. In this paper, we report the development of new tools that allowed us to test this prediction. Specifically, we generated biologically active fluorophore-tagged WNT1, PORCN, and WLS. We further show that co-expression of WLS with WNT1 allows the visualization of WNT1 on the cell surface and in cellular projections in both cultured cells and developing embryos.

2. Materials and methods

Many thanks to Dr. Rami N. Hannoush of Genentech for providing Alk-C16 palmitate. We would also like to thank Dr. Erik Snapp (Albert Einstein University) for the cDNA encoding moxGFP and Dr. David Turner (University of Michigan) for the membrane-tethered eGFP construct (GFP-CAAX). Thanks also to Dr. Randy Moon (University of Washington) for providing Super8xTopflash, Super8xFopflash and RL-CMV, Dr. Elena Frolova (University of Alabama – Birmingham) for a partial chick Wnt1 cDNA, Dr. Jennifer Lippincott-Schwartz for GalT-GFP, Dr. Tatsuhiko Kadowaki (Xi'an Jiaotong-Liverpool University) for mPORCND and Dr. Roel Nusse for LSL cells (L cells stably transfected with TOPFLASH and LacZ constructs).

2.1. Materials and vendors

Fetal Bovine Serum (Atlanta Biologicals); Alk-C16 (Cayman Chemical); Rabbit anti-DsRed (Clontech); DMEM, 200 mM L-Glutamine (Corning); 96-Well White Solid Plates Tissue culture treated (Costar); 100xPenstrep (Corning); pCDNA3.1 (Invitrogen); anti-mouse Alexa Fluor® 647, anti-rabbit Alexa Fluor® 488 (Jackson ImmunoResearch); IRDYE® 680RD Goat anti-Rabbit, Streptavidin IR800 (LI-COR); biotin azide, anti-mouse Alexa Fluor® 680 (Life Technologies); mouse anti-HA (Millipore); fertile eggs (Petaluma Farms); Protein A/G beads (Pierce); Fugene HD, Dual-Luciferase Reporter Assay (Promega); and Dual-Light Luciferase and β-galactosidase Reporter Kit, SlowFade® Gold antifade reagent (Thermo Scientific).

2.2. Constructs

Full-length cDNAs encoding chick WNT1 is not available. Thus, we have created fusion proteins consisting of mouse sequences for the signal peptide and chick sequences for the remainder of the protein. As the mature protein is mostly chick derived, we refer to this construct as cWNT1. For the cWNT1 construct, mouse sequences encoding amino acid 1–63 (MGLWAL...EPSLQL) were appended to chick sequences for amino acid 64–370 (LSRKQR...VLHECL). Similarly, for the chick WNT3A (cWNT3A) construct, mouse sequences encoding amino acid 1–24 (MAPLGY...SYPIWW) were appended to chick sequences for amino acids 24–352 (SLAIGH...).

N-terminally tagged cWNT1 was generated by inserting tags after the signal peptide cleavage site, between amino acids 34 and 35. C-terminally tagged Wnts, including cWNT1-moxGFP, cWNT1-eGFP, cWNT3A-moxGFP, and mWNT7a-moxGFP, were generated by appending 1–3 linkers (SGGGGS) at the C-terminus of the Wnt protein. For zWnt1-eGFP, the linker was SGGGS. The linker sequences are followed by those encoding either moxGFP or eGFP. For cWNT1-Fc, the sequences surrounding the junction between cWNT1, vector sequences, and Fc encode a fusion protein with the following residues: [...VLHECL-DPDDDDKDPEE-PKSCDKT...]. The relevant sequences for zWnt1-Fc are [...TVHQCL-DDPDDDDKDPEE-PKSCDKT...].

mPORCN variant D and chick WLS were used for our studies. PORCN and WLS were tagged on the C-terminus with mCherry. For PORCN, the amino acids surrounding the junction are [...FYRLIG- GT-MVSKGEE...]. For WLS, the amino acids surrounding the junction are [...ARKEAQE-SA-MVSKGEE...].

spGFP:WNT1 (209–239) was used as a substrate in some palmitoylation assays and is described in an earlier publication (Miranda et al., 2014).

All inserts were subcloned into pCDNA3.1 for expression in cultured cells and a variant of pCIG (lacking the nuclear GFP) for expression in chick embryos (Megason and McMahon, 2002).

2.3. Cell Culture

COS7, HEK293T and L cells were grown in standard medium (DMEM supplemented with 10% fetal bovine serum, 4 mM L-glutamine, and 1x penicillin/streptomycin) on 100 mm plates in humidified incubators set to 10% CO_2 (COS7 and HEK293T) or 5% CO_2 (L cells).

2.4. Paracrine/juxtacrine TopFlash assay

We have previously reported the generation of L cells stably transfected with empty vector (LMock) and cWNT1 (LWNT1) (Galli and Burrus, 2011). LMock and LWNT1 cells were split to a 96 well white tissue culture assay plate at 2500 cells/well in volume of 100 µl and incubated for 48 h. Media from the LMock and LWNT1 cells were transferred to new wells in the assay plate. LSL reporter cells (Mikels and Nusse, 2006b) were then added (25,000 cells/well) to the wells containing LMock or LWNT1 cells and wells containing conditioned media from LMock or LWNT1 cells. The cultures were incubated for approximately 21hrs before assaying for Wnt activity using the Dual-Light Luciferase Kit. Luciferase measurements were carried out in a MicroLumatPlus LB96V Microplate Luminometer.

2.5. Autocrine SuperTopFlash assay

Fugene HD was used to transfect HEK293T with pCDNA3.1 expression constructs along with 8XSuperTopFlash constructs (Veeman et al., 2003). pCDNA3.1 constructs were transfected at 0.25 μg/well; 8XSuperTopFlash or 8XSuperFopFlash were used at 0.01 μg/well; and RL-CMV was used at 0.01 ng/well. Cells were incubated overnight, lysed and measured as per the Dual-Luciferase Reporter Assay protocol (Promega). Luciferase measurements were collected using a TD- 20/20 luminometer.

2.6. Palmitoylation assay

Fugene HD was used to transfect HEK293T cells with pCDNA3 or 3.1 expression constructs in a 6 well plate. WNT1-Fc or spGFP:WNT1 (209–239)-Fc was expressed as the palmitoylation substrate. PORCN (mouse PORCN variant D) was expressed as the palmitoyl acyl transferase while GFP was used as a control. Transfected cells were metabolically labeled with 100 μM ω-Alkyne palmitic acid (Alk-C16) for 20–24 h. Cells were lysed in 100 mM sodium phosphate, pH7.5 containing 150 mM NaCl, 1% NP-40, and 1X Halt protease and phosphatase inhibitor cocktail before immunoprecipitating Fc containing fusions with Protein A/G beads. Proteins retained on the beads were subjected to click chemistry with biotin azide before subjecting them to SDS-PAGE and analysis by Western blot. Western blots were probed with IRDye800 conjugated streptavidin, and anti-WNT1 antibodies followed by goat Alexa Fluor® 680-conjugated anti-mouse secondary antibody before analyzing with an Odyssey CLX infrared scanner.

2.7. Western blots

HEK293T cells were transfected with the appropriate pcDNA3.1 expression constructs and incubated overnight. The next day the cells were lysed, separated by SDS-PAGE in a 10% gel and analyzed by Western Blot. The blot was probed with anti-cWnt1, anti-GFP, and anti-DsRed antibodies followed by anti-mouse Alexa Fluor® 680 or IRDYE® 680RD Goat anti-Rabbit. Western Blots were scanned and analyzed on an Odyssey CLx scanner.

2.8. Staining and imaging fixed cells

COS7 cells were transfected with Fugene HD according to manufactures protocol with pCDNA3.1 expression constructs encoding cWNT1, cWNT1-moxGFP, PORCN, and PORCN-mCherry in a 24 well plate and incubated overnight. Cells were split onto 8-chamber glass slides and incubated overnight. Cell were then washed with PBS, fixed with 4% paraformaldehyde, permeabilized with PBS containing 1% TX-100, blocked in blocking buffer (PBS containing 3% sheep serum and 0.1% Tween) and then probed with mouse anti-cWnt1 or rabbit anti-PORCN antibodies. Cells were incubated overnight at 4 °C. The following day, cells were incubated with blocking buffer containing DAPI and anti-mouse Alexa Fluor® 647 or anti-rabbit Alexa Fluor® 488 secondary antibodies. Cells were mounted in SlowFade® Gold antifade reagent and imaged on a Zeiss LSM 710 with the 63x Oil objective (Plan Apochromat). Images were processed in Photoshop.

2.9. Live cell imaging

COS7 cells were transfected with pCDNA3.1 expression constructs encoding cWNT1-moxGFP, PORCN-mCherry, WLS-mCherry, and/or eGFP-CAAX in a 35 mm plate using Fugene HD according to manufacturer's protocol. The cells were incubated overnight and imaged live on a Zeiss LSM 710 with the 63x dipping objective at room temperature. Images were processed in Adobe Photoshop (version CS6).

2.10. In ovo electroporation and live imaging of chick embryos

Rhode Island Red chicken eggs were incubated to Hamburger and Hamilton (HH) stage 13–14 (Hamburger and Hamilton, 1951). The eggs were windowed and injected with India Ink for visualization. A small section of the vitelline membrane was torn near somite I to allow access to the spinal cord. The embryos were then injected with one or more DNA constructs in a solution containing 0.38% methyl cellulose and 0.19 mg/ml Fast Green. Immediately after injection, the embryo was electroporated with 4 × 50 ms pulses at 52–55 V. A piece of parafilm was placed between the embryo and the electrodes to prevent damage to the tissue (Galli et al., 2016a). The embryos were overlaid with 1X Pen/Strep (to prevent bacterial growth), resealed, and incubated for an additional 21–24 h to HH stages 17–18.

2.11. Live imaging of chick embryos

Successfully electroporated embryos were harvested at HH stage 17–18 and placed dorsal side up in a small well made of 3 layers of electrical tape on a microscope slide. Embryos were bathed in DMEM supplemented with 10% FBS and 4 mM L-glutamine and overlaid with a coverslip. Images of the dorsal region of the spinal cord were then collected using confocal microscopy. All imaging was performed on a Zeiss LSM 710 confocal microscope using lasers at 488 nm and 543 nm. 63x oil (Plan Apochromat) and water dipping (W N-Acroplan) objectives were used. Images were collected using ZEN software.

2.12. Statistical analysis

The significance of our data was evaluated using one-way ANOVA with Tukey HSD.

3. Results

3.1. Cell contact promotes WNT1 signaling

It has long been appreciated that Wnts are poorly secreted. Thus, the finding that L cells secrete WNT3A at low, but appreciable, levels was significant in that it opened the door for the purification and manipulation of Wnt proteins (Shibamoto et al., 1998; Willert et al., 2003). Because of the success of expressing Wnts in L cells, our lab generated L cells expressing cWNT1 (Galli and Burrus, 2011). Biologically active cWNT1 is present in the conditioned media from these cells; however, our studies show that it is present at exceedingly low levels (Galli and Burrus, 2011). To assess the relative contribution of paracrine versus juxtacrine signaling in L cells, we compared the ability of WNT1 conditioned media and LWNT1 cells to promote signaling in LSL reporter cells (Mikels and Nusse, 2006b). Consistent with the idea that WNT1 localized to the cell surface or filopodia plays an important role in signaling, we found that the incubation LWNT1 cells with LSL cells (paracrine + juxtacrine signaling) induced over 100 fold more signaling than did LWNT1 conditioned media with LSL cells (paracrine signaling) (Fig. 1). Thus, we conclude that the vast majority of bioavailable cWNT1 is cell associated.

3.2. WNT1-Fc is expressed as a biologically active and intact protein that can be used for palmitoylation assays

The palmiteoylation of Wnts is critical for membrane trafficking and receptor binding (Doubravska et al., 2011; Galli and Burrus, 2011; Galli et al., 2016b; Gao and Hannoush, 2014b; Komekado et al., 2007; Kurayoshi et al., 2007; Miranda et al., 2014; Takada et al., 2006). The advent of a click chemistry palmitoylation assay has made it possible for us to quantitatively monitor Wnt palmitoylation (Chen et al., 2009; Hannoush and Arenas-Ramirez, 2009; Hannoush and Sun, 2010). In

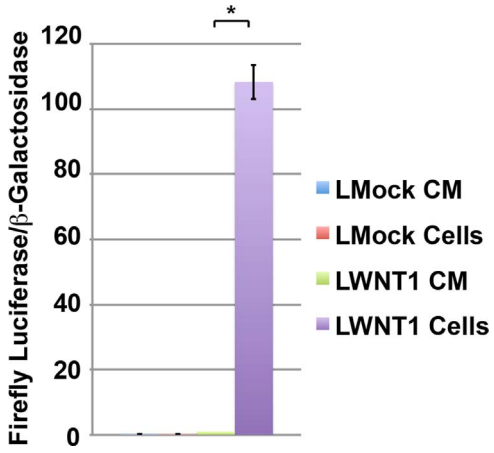

Fig. 1. Cell contact dramatically increases paracrine WNT1 signaling. For this assay, LMock (control) and LWNT1 cells were cultured to confluence. Either conditioned media (CM) or cells were incubated in wells containing LSL reporter cells as described in materials and methods. Wnt signaling was assessed via activation of a reporter construct harboring 8 TCF binding sites upstream of the cDNA encoding Firefly Luciferase (Mikels and Nusse, 2006a). Data were normalized to the constitutive expression of β-galactosidase. Each data point reflects the average of 8 independent replicates. Error bars +/- standard error. The asterisk indicates that $p < 0.01$.

this assay, cells transiently transfected with Wnt and PORCN expression constructs are metabolically labeled with alkyne palmitate (C16-Alk). Wnt is immunoprecipitated prior to carrying out "click chemistry", which results in the covalent linkage of biotin azide to alkyne palmitate labeled Wnt. While it is possible to carry out this assay using untagged Wnt proteins (Gao et al., 2011; Gao and Hannoush, 2014a, 2014b; Hannoush and Arenas-Ramirez, 2009; Hannoush and Sun, 2010), we and others have used Fc-tagged Wnt fusions for this assay (Chen et al., 2009; Miranda et al., 2014). However, it was not known if Fc-tagged WNT1 retained its ability to signal.

To demonstrate the ability of cWNT1-Fc to be palmitoylated by PORCN, we carried out a click chemistry palmitoylation assay. HEK293T cells were transiently transfected with cWNT1-Fc along with either GFP (control) or PORCN and metabolically labeled with DMSO (control) or alkyne palmitate. After precipitating cWNT1-Fc from cell lysates, biotin was then covalently linked to the alkyne palmitate using the click chemistry reaction. Western blot analysis using anti-cWNT1 antibodies shows that cWNT1-Fc was effectively precipitated from all samples (Fig. 2A). Blotting with streptavidin shows the presence of palmitoylated cWNT1-Fc in all samples treated with alkyne palmitate (Fig. 2A). Because PORCN is ubiquitously expressed at low levels, we were not surprised to see low levels of palmitoylation in the absence of transfected PORCN (Fig. 2A). As expected, co-transfection with PORCN increased the levels of palmitoylation (Fig. 2A). Thus, cWNT1-Fc can serve as a substrate in a PORCN-dependent palmitoylation assay.

We then proceeded to test the biological activity and integrity of the cWNT1-Fc fusion. To test whether the cWNT1-Fc fusion proteins retained the ability to signal, we carried out a Super8XTopFlash reporter assay in transiently transfected HEK293T cells. This assay shows that cWNT1-Fc is fully active, exhibiting 1.5 fold more activity that wild-type cWNT1 (Fig. 2B). As we have not quantified the actual levels of WNT1 protein in cells transfected with cWNT1 or cWNT1-Fc, we cannot conclude that this difference can be attributed to an increase in the signaling potency of cWNT1-Fc.

To test whether the cWNT1-Fc fusion is expressed as a full-length protein, we used Western blot analysis to assess the integrity of the WNT1-Fc overexpressed in HEK293T cells. Consistent with the reported sizes of mWNT1 (39–48 kDa) and IgG Fc (32 kDa), our data show that the apparent molecular masses of cWNT1 and WNT1-Fc range between 39 and 48 kDa and 72–81 kDa, respectively (Fig. 2C). The multiple bands observed for cWNT1and WNT-Fc are consistent with previously published reports demonstrating that WNT1 is differentially glycosylated (Brown et al., 1987; Burrus and McMahon, 1995). Thus, the cWNT1-Fc fusion is a highly useful tool for a variety of assays, including palmitoylation assays.

3.3. *WNT1-GFP is expressed as a biologically active and intact protein*

Our success with tagging cWNT1 with the Fc domain led us to wonder whether we might also be able to tag cWNT1 with fluorescent proteins. To test this, we first generated cWNT1 with C-terminal moxGFP, eGFP, mCherry, or mKate2 tags (Costantini et al., 2015;

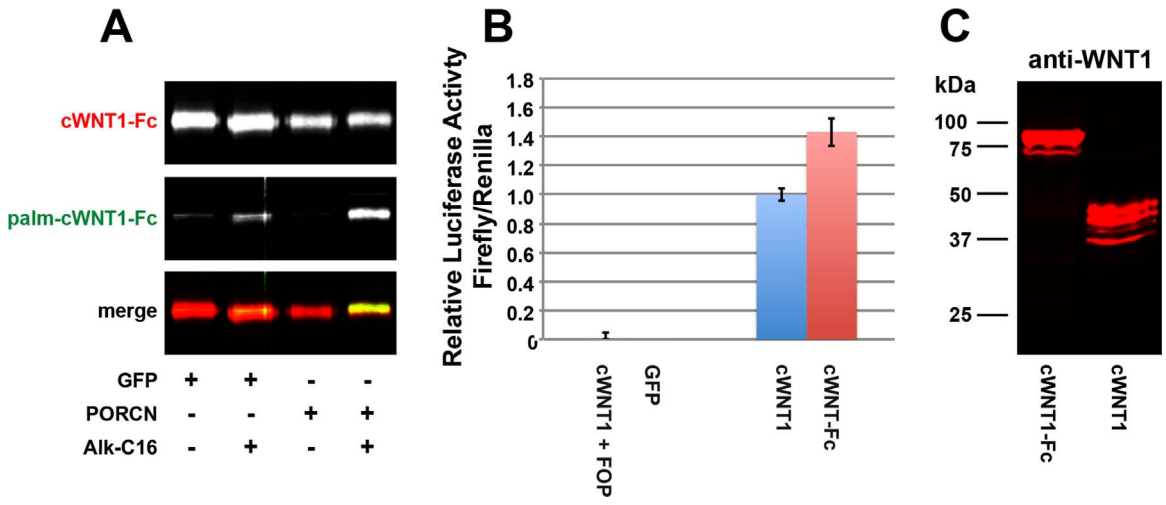

Fig. 2. cWNT1-Fc is an intact biologically active fusion protein that can serve as a substrate for palmitoylation assays. A) For the palmitoylation assay, HEK293T cells were transiently transfected with cWNT1-Fc along with GFP (control) or PORCN. Cells were metabolically labeled with DMSO (D, control) or Alkyne-palmitate. WNT1-Fc was precipitated from cell lysates using A/G Agarose beads and subjected to click chemistry to covalently attach biotin azide to the alkyne palmitate. Proteins were separated by SDS-PAGE and analyzed by probing immunoblots with anti-WNT1 followed by an Alexa Fluor 680 labeled secondary antibody (red) and Streptavidin IR 800 dye (green). The data shown are representative of 3 independent replicates. **B)** The biological activity of cWNT1 and cWNT1-Fc was compared in an autocrine SuperTopFlash assay as described in Materials and Methods. HEK293T cells were transfected with GFP along with the indicated plasmid. GFP levels were varied such that total DNA levels were held constant. Data from cells transfected with GFP and cWNT1 were normalized to a value of 1. Each data point represents the average of 10–30 independent replicates carried out on 2–6 different days. Errors bars indicate +/- standard error. **C)** HEK293T cells were transiently transfected with cWNT1 or cWNT1-Fc. Cell lysates were subjected to SDS-PAGE and Western blot analysis using anti-cWNT1 monoclonal antibodies developed in our laboratory followed by an Alexa Fluor 680 labeled secondary antibody (red). Images were collected using a Licor CLX Odyssey scanner.

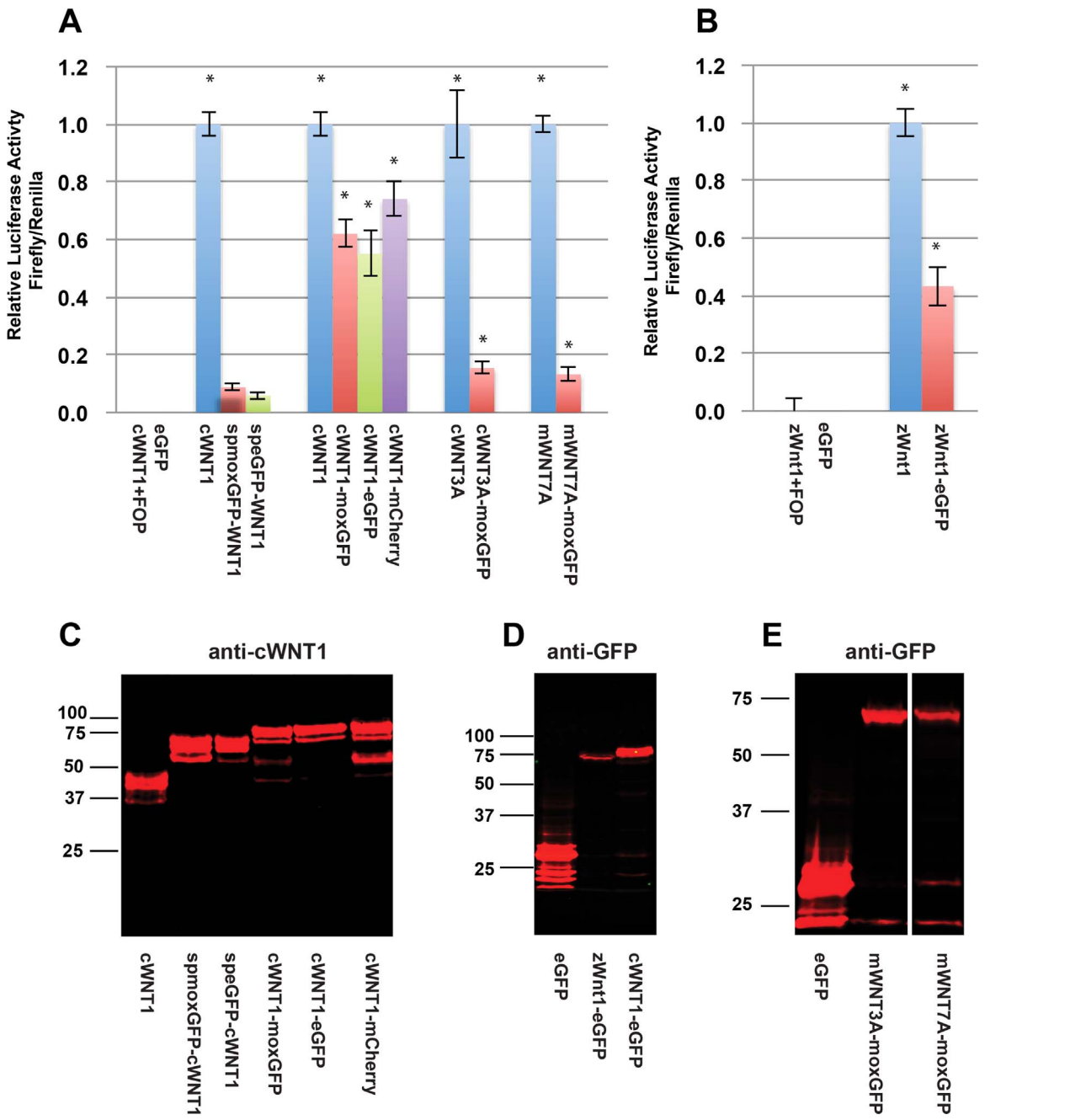

Fig. 3. WNT1-GFP fusions are expressed as full-length proteins and are biologically active. A and B) The autocrine SuperTopFlash assay was carried out as described in Experimental Procedures. HEK293T cells were transfected with the indicated plasmid. Constructs in which the fluorophore is listed before the Wnt are tagged on the N-terminus while those in which the fluorophore is listed after the Wnt are tagged on the C-terminus. DNA levels were held constant. For this graph, data from cells transfected with GFP alone (endogenous Wnt signaling) were set at zero while data from cells transfected with chick WNT1 (A) and zebrafish WNT1 (B) were normalized to a value of 1. Each data point represents the average of 15–80 independent replicates. Errors bars indicate +/- standard error. The asterisk indicates $p < 0.01$ as compared to cell transfected with GFP alone. **C-E)** HEK293T cells were transfected with the indicated constructs. Cell lysates were subjected to SDS-PAGE followed by Western blot analysis. In C, blots were probed with anti-cWNT1 antibodies while in D and E, blots were probed with anti-GFP antibodies. Alexa Fluor 680 labeled secondary antibody (red) was used for all blots. Images were collected using a Licor CLX Odyssey scanner.

Shcherbo et al., 2009). An SGGGGS linker was included in between the cWNT1 and fluorophore in order to promote flexibility (Chen et al., 2013). As it had been previously reported that the presence of cysteine residues in V5 tags was deleterious to Wnt activity, we chose to utilize both eGFP and a variant of GFP with no cysteine residues (moxGFP) for our studies with cWNT1 (Costantini et al., 2015; MacDonald et al., 2014). For the sake of comparison, we also generated N-terminally tagged cWNT1, in which the GFP tag was situated after the signal peptide and its predicted cleavage site. We then tested the biological activity of these cWNT1 fusions in an 8XSuperTopFlash reporter assay (Fig. 3A). Overexpression of wild-type cWNT1 causes a roughly 200 fold increase in signaling as compared to GFP alone (data not shown). Our data further show that cWNT1 fusions bearing C-terminal GFP and mCherry tags retained 60–70% of wild-type activity. However, the cWNT1-mKate2 fusion retained little or no activity (data not shown). The inclusion of 2X and 3X SGGGGS linkers between cWNT1 and moxGFP did not significantly improve the biological activity as compared to a single linker (data not shown). To test whether WNT1 from other species could tolerate a C-terminal tag, we then tested the biological activity of zWnt1-eGFP. zWnt1-eGFP also retained just over

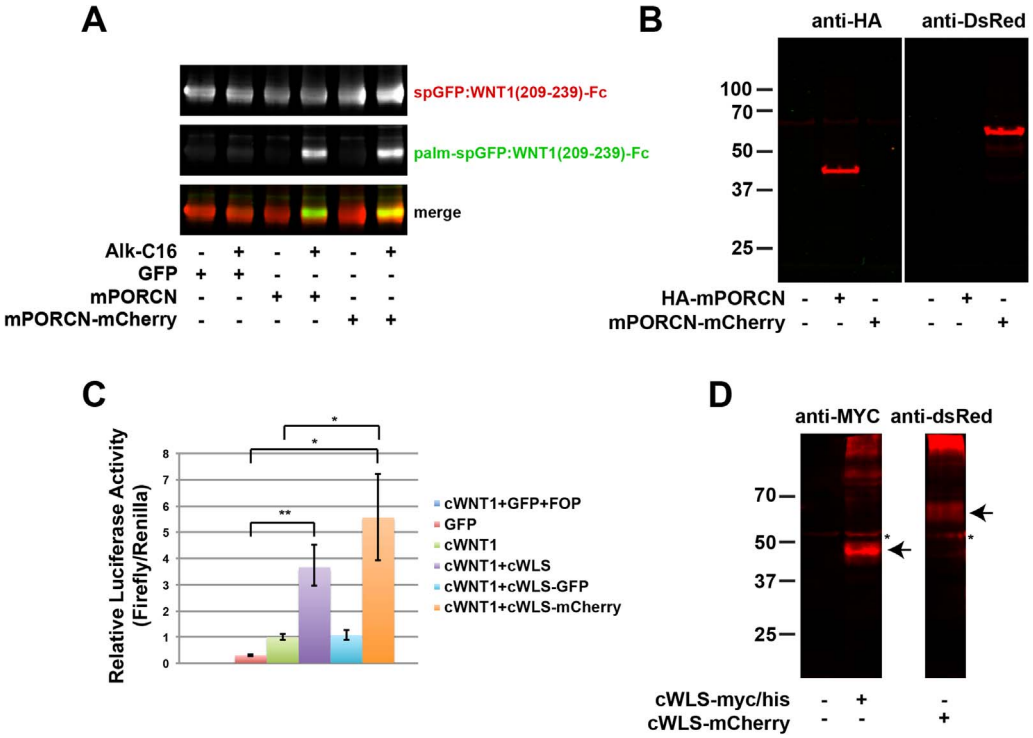

Fig. 4. mCherry tagged variants of PORCN and WLS are functional and expressed as full-length proteins. A) The enzymatic activity of PORCN-mCherry was compared to untagged PORCN in a click chemistry based palmitoylation assay. HEK293T cells were transiently transfected with a WNT1 palmitoylation substrate (spGFP:WNT1(209–239)-Fc) along with GFP (negative control), untagged PORCN or PORCN-mCherry. Cells were metabolically labeled with DMSO (-Alk-C16) or Alkyne-palmitate (+Alk-C16). spGFP:WNT1(209–239)-Fc was precipitated from cell lysates using A/G Agarose beads and subjected to click chemistry to covalently attach biotin azide to the alkyne palmitate. Proteins were separated by SDS-PAGE and analyzed by probing immunoblots with anti-WNT1 and Alexa Fluor 680 labeled secondary antibody to detect WNT1 (red) and Streptavidin IR 800 dye to detect alkyne palmitate (green). The data shown are representative of 2 independent replicates. B) HEK293T cells were transiently transfected with HA-PORCN or PORCN-mCherry. Cell lysates were subjected to SDS-PAGE and Western blot analysis. The HA-PORCN blot was probed with anti-HA followed by Alexa Fluor 680 labeled secondary while the PORCN-mCherry was probed with anti-DsRed followed by Alexa Fluor 680 labeled secondary. Blots were imaged using a Licor CLX Odyssey scanner. **C)** An autocrine assay for WNT1 signaling was carried out as described in materials and methods. Briefly, HEK293T cells were transfected with GFP, cWNT1, and/or WLS (tagged and untagged variants). Cells were also transfected with 8XSuperTopFlash, a reporter construct in which the expression of firefly luciferase is driven by 8X TCF binding sites. The 8XSuperFopFlash is used as a negative control and has mutations in the TCF binding sites. Renilla Luciferase is expressed under the control of a constitutive promoter. Data shown represent 15–20 independent replicates from 3 to 4 days. Error bars represent +/- standard error. * indicates $p < 0.01$ while ** indicates $p < 0.05$ **D)** HEK293T cells were transiently transfected with WLS-myc/his or WLS-mCherry. Cell lysates were subjected to SDS-PAGE and Western blot analysis. The WLS-myc/his blot was probed with anti-myc followed by Alexa Fluor 680 labeled secondary while the WLS-mCherry was probed with anti-DsRed followed by Alexa Fluor 680 labeled secondary. Blots were imaged using a Licor CLX Odyssey scanner. Arrowheads show the position of the tagged WLS protein. The asterisk denotes a non-specific band found in all samples, including mock transfected cells.

40% biological activity (Fig. 3B), thus demonstrating that this approach is viable for Wnts derived from different vertebrate species. The addition of a N-terminal GFP tags to cWNT1 yielded fusion proteins with no significant activity as compared to GFP (Fig. 3A).

Western blot analysis showed variable levels of degradation amongst the newly generated fusion proteins (Fig. 3C-E). Consistent with previous reports that WNT1 is differentially glycosylated (Brown et al., 1987; Burrus and McMahon, 1995), Western blot analysis using highly specific anti-cWNT1 antibodies developed in our lab show the presence of multiple bands ranging from 38 to 49 kDa (Fig. 3C). Fig. 3C). The molecular size of the C-terminal fusions agrees well with our predictions; however, that of the N-terminal fusions does not. The N-terminal GFP-cWNT1 fusions (with eGFP and moxGFP) migrated between 56 and 68 kDa while the C-terminal GFP and mCherry fusions for chick and zebrafish WNT1 migrated between 69 and 76 kDa (Fig. 3C,D). Though both fusions have a predicted mass of ~ 68 kDa, it is notable that the C-terminal fusions migrate at an apparent mass that is roughly 14 kDa larger than the N-terminal fusions. We do not know if the reduced apparent size of the N-terminal fusion represents degradation, use of an alternate signal peptide cleavage site, or aberrant migration due to structural differences. Nonetheless, we think it likely that the reduced apparent mass of the fusion is linked to the failure of the N-terminally tagged WNT1 fusions to signal.

While the chick and zebrafish WNT1-eGFP fusion showed virtually no degradation, the moxGFP-tagged cWNT1 exhibited consistent, but very low, levels of degradation (Fig. 3C,D). By contrast, mCherry-tagged cWNT1 showed significant levels of degradation (Fig. 3C).

To determine whether our ability to generate functional fluorophore-tagged WNT1 could be extended to additional Wnt homologues that signal via the β-catenin dependent pathway, we then tagged both cWNT3A and mWNT7A with moxGFP at the C-terminus (after an SGGGGS linker) (Fig. 3D). Though the fusions do retain statistically significant signaling capacity, the activity of the tagged cWNT3A and mWNT7A variants was unacceptable as it was less than 20% of the wild-type proteins. Thus, consistent with results with other labs, we find that the ability of different Wnt family members to tolerate C-terminal tags is quite variable (Holzer et al., 2012; Luz et al., 2014; Stanganello et al., 2015).

The generation of C-terminally GFP-tagged chick and zebrafish WNT1 that is expressed as a full-length protein and retains biological activity represents a significant advance in the Wnt field.

3.4. PORCN-mCherry and WLS-mCherry are expressed biologically active proteins

PORCN and WLS are critical players for the membrane trafficking and transport of Wnt proteins to target cells. To add to our growing toolbox, we next sought to generate fluorophore-tagged PORCN and WLS fusions. To test the biological activity of PORCN, we compared the ability of wild-type PORCN and PORCN-mCherry to promote the

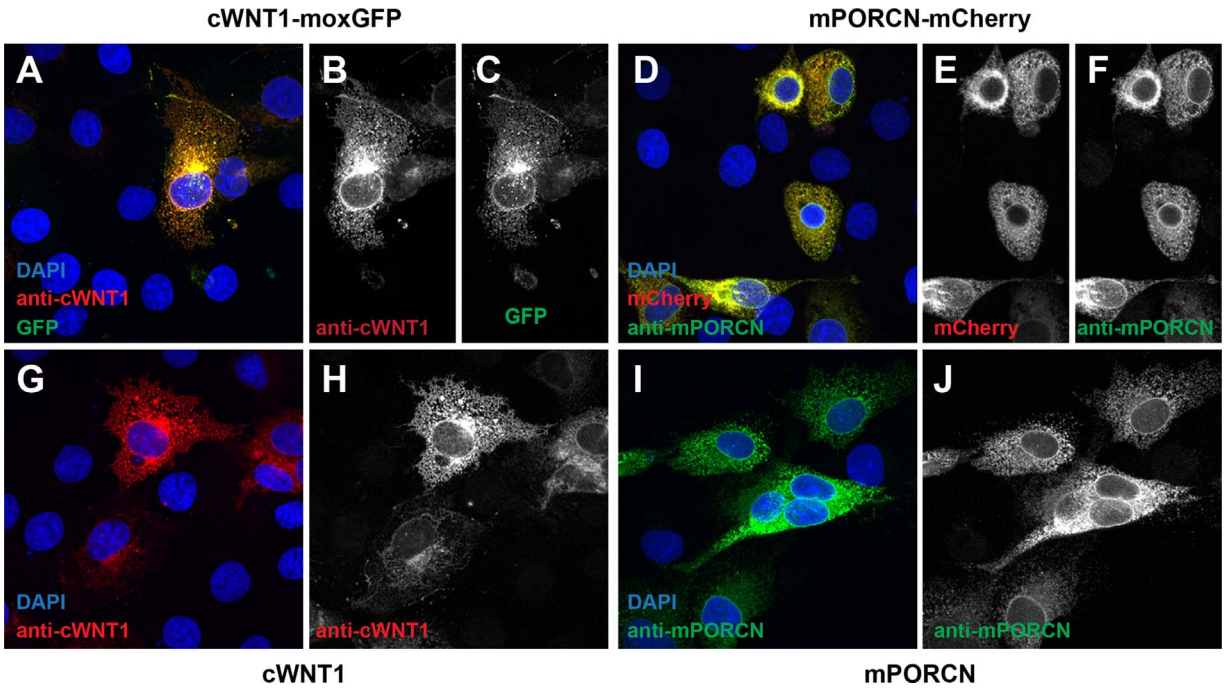

Fig. 5. The subcellular localization of tagged and untagged versions of chick WNT1 and mouse PORCN are nearly identical. COS7 cells were transiently transfected with cWNT1-moxGFP (A-C), cWNT1 (G-H), mPORCN-mCherry (D-F) or mPORCN (I-J). Cells were fixed, counterstained with DAPI (blue) and immunostained with the indicated antibodies. Images were collected by confocal microscopy.

addition of alkyne palmitate to spGFP:WNT1 (209–239)-Fc, a WNT1 palmitoylation substrate developed in our lab (Miranda et al., 2014). Our results show that PORCN-mCherry was comparable to wild-type PORCN in its ability to promote the palmitoylation of spGFP:WNT1 (209–239)-Fc (Fig. 4A). Western blot analysis was then used to assess the integrity of the PORCN-mCherry fusion (Fig. 4B). As a control, we first assessed the migration of PORCN-HA. Although the predicted molecular weight of PORCN-HA is 57 kDa, our data show that it migrates at roughly 46 kDa (Fig. 4B). Analysis of untagged PORCN using anti-PORCN antibodies also indicates that it runs at a smaller apparent molecular weight than predicted (data not shown). PORCN-mCherry migrates as a single band at approximately 64 kDa, which is close to the expected weight of 68 kDa (46 kDa PORCN-HA with the addition of mCherry (27 kDa) and the loss of HA (5 kDa)) (Fig. 4B). As we do not observe any degradation products, we think it likely that this fusion represents an intact protein. In sum, PORCN-mCherry is expressed as a biologically active protein.

To test the biological activity of WLS fusions, we took advantage of the observation that co-expression of WLS along with WNT1 increases WNT1 signaling output as compared to WNT1 alone in an 8xSupertopFlash reporter assay (Galli et al., 2016b). Thus, we

tested the ability of wild-type WLS, WLS-eGFP, WLS-mKate2, and WLS-mCherry to enhance WNT1 signaling. Consistent with our previous publication, co-transfection of WLS along with cWNT1 enhanced signaling 3.7 fold as compared to cWNT1 alone (Fig. 4C) (Galli et al., 2016b). WLS-eGFP and WLS-mKate2 failed to promote cWNT1 signaling (Fig. 4C and data not shown). WLS-mCherry, however, significantly enhanced cWNT1 signaling ($p < 0.01$) at levels comparable to that of wild-type WLS (Fig. 4C). The predicted size of cWLS is 62 kDa. However, Western blot analysis shows that WLS-myc/his migrates further than expected, with an apparent molecular mass of 48 kDa while WLS-mCherry is 76 kDa (Fig. 4D). The presence of higher molecular weight bands near the top of the blot is consistent with a recent report demonstrating the multimerization of WLS (Petko et al., 2017). Thus, WLS-mCherry is expressed as a biologically active and intact protein.

In sum, we have successfully engineered biologically active and intact PORCN-mCherry and WLS-mCherry fusions.

3.5. *WNT1-GFP and PORCN-mCherry fusions replicate the subcellular localization of untagged protein in fixed cultured cells*

To provide further evidence that the fusion proteins are expressed as intact proteins, we overexpressed cWNT1-moxGFP or mPORCN-mCherry and compared the subcellular localization of the antibody epitope and the fluorophore. The presence of yellow in the merged image (Fig. 5A) indicates nearly complete overlap in the signal from the cWNT1 epitope (Fig. 5B) and the fluorescent signal from the GFP (Fig. 5C). Parallel experiments with PORCN also show extensive colocalization between the epitope and the mCherry (Fig. 5D-F). The one exception is that our antibody stains an epitope in the perinuclear region that is not labeled with mCherry. Additional controls show that this perinuclear staining is the result of non-specific staining (data not shown). In sum, the colocalization of the WNT1 and PORCN epitopes with the fluorophore provides additional evidence that the tagged variants are expressed as intact proteins.

Because the addition of tags to proteins can cause artifacts in the subcellular localization of these proteins, we also compared the localization of untagged and fluorophore-tagged variants of cWNT1 and PORCN overexpressed in COS7 cells. The untagged and tagged variants were detected using antibodies developed in our lab (Galli et al., 2007; Galli and Burrus, 2011). Consistent with previous studies showing the localization of WNT1 and PORCN to the endoplasmic reticulum, we found that untagged and fluorophore-tagged variants of WNT1 and PORCN were distributed in a reticulated pattern that extended throughout the cell (Fig. 5A-B,D-E, G-J). This reticulated pattern mirrored that of spGFP-KDEL, a GFP variant that resides in the endoplasmic reticulum (data not shown). Given the similarities in the subcellular localization between tagged and untagged variants of WNT1 and PORCN, we conclude that the WNT1-moxGFP and PORCN-mCherry fusions faithfully report the subcellular localization of the WNT1 and PORCN. Note that we were unable to carry out similar studies for WLS as we did not have access to anti-WLS antibodies that recognize chick WLS.

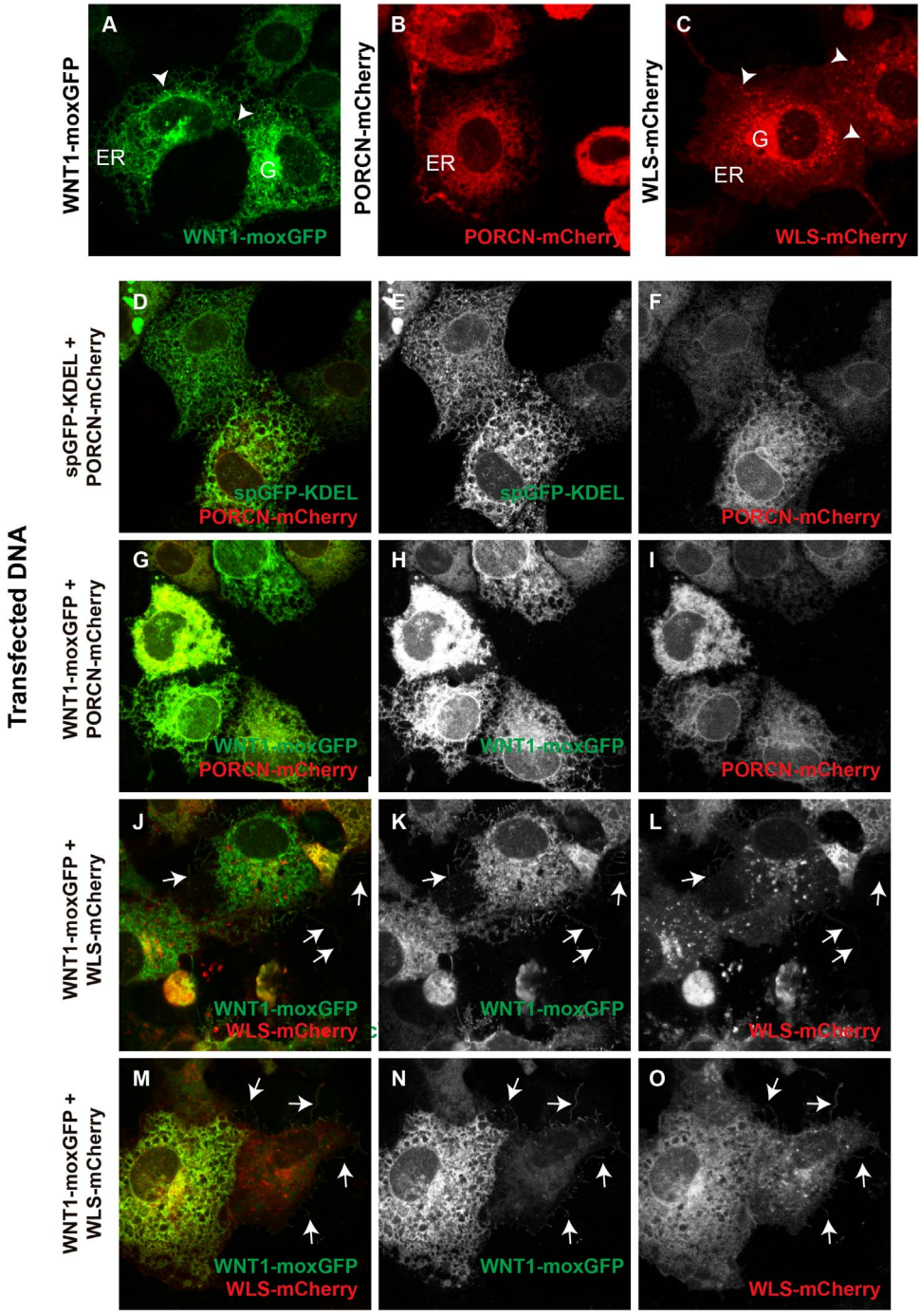

Fig. 6. Co-expression of WLS-mCherry, but not PORCN-mCherry, causes a redistribution of cWNT1-moxGFP from the endoplasmic reticulum to the cell surface and cellular projections in live cultured cells. COS7 cells were transiently transfected with the indicated constructs and imaged live using Zeiss LSM 710 confocal microscope outfitted with a water dipping 63X objective. Arrowheads show the presence of punctae; arrows mark cellular projections.

3.6. WLS-mCherry, but not PORCN-mCherry, causes a redistribution of WNT1-moxGFP in cultured COS7 cells

To test the utility of cWNT1-moxGFP, PORCN-mCherry, and WLS-mCherry, we carried out live imaging of COS7 cells, which were transiently transfected with different combinations of fusion proteins (Fig. 6). Consistent with our data from fixed cells, cWNT1-moxGFP is primarily localized to the endoplasmic reticulum and the Golgi apparatus (Fig. 6A). Small vesicle-like punctae were also observed (Fig. 6A). Like cWNT1-moxGFP, PORCN-mCherry was also found in the ER (Fig. 6B). However, it was not apparent in the Golgi or in punctae (Fig. 6C). WLS-mCherry was faintly visible in the endoplasmic reticulum, with more pronounced staining in the Golgi (Fig. 6C). GalT-GFP was used to confirm the identification of the Golgi (data not shown). Consistent with its role as a cargo transporter, WLS-mCherry was also observed in vesicle-like punctae (Fig. 6C). Very faint fluorescence was also observed around the perimeter of the cell and in cellular projections (Fig. 6C).

Previous studies from our lab show that although overexpression of PORCN or WLS causes an increase in the levels of WNT1 on the cell surface, only WLS significantly enhances WNT1 signaling (Galli et al., 2016b). To test the effects of PORCN or WLS on the distribution of WNT1, we co-transfected PORCN-mCherry or WLS-mCherry along with WNT1-moxGFP and carried out imaging in live cells. Although

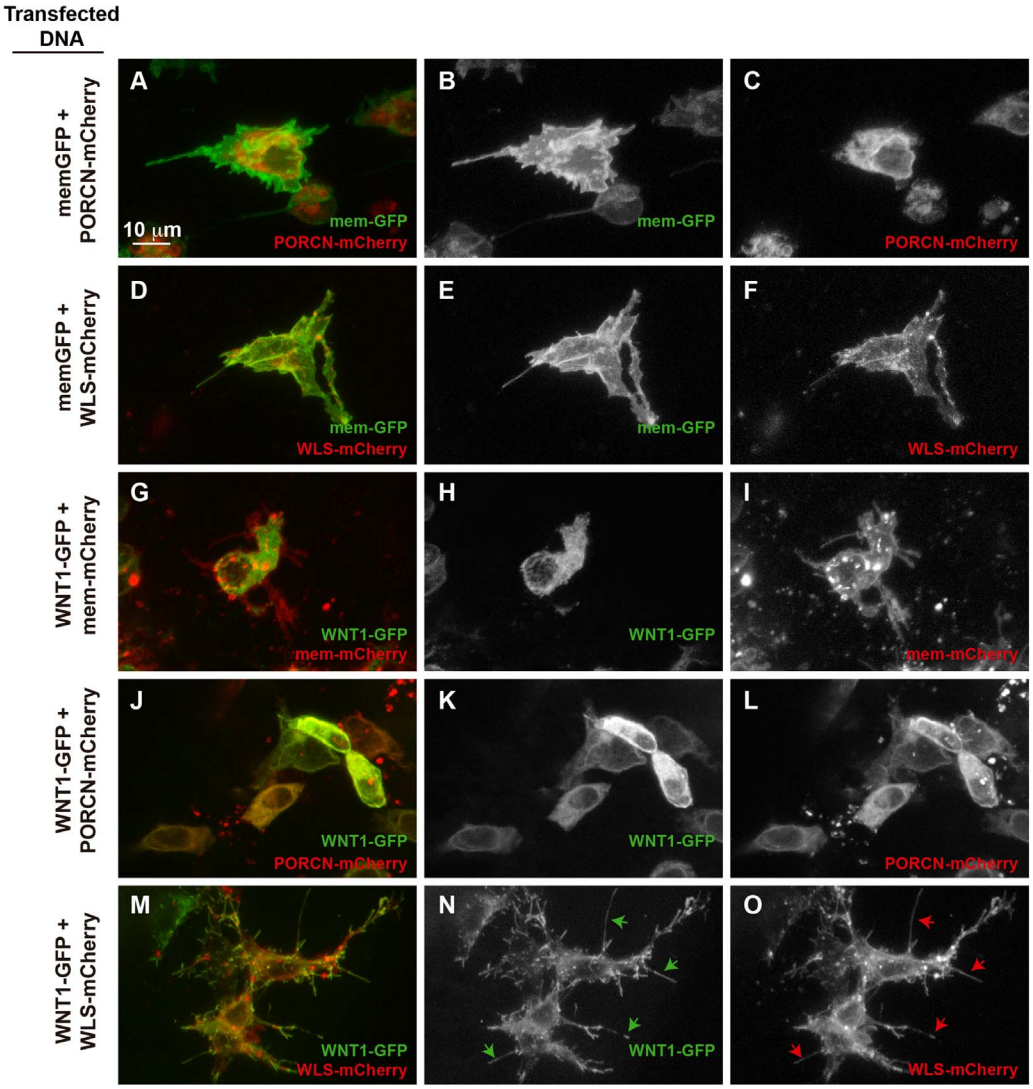

Fig. 7. Co-expression of WLS-mCherry, but not PORCN-mCherry, causes a redistribution of WNT1-moxGFP from the endoplasmic reticulum to the cell surface and cellular projections in developing neural crest cells. Chick embryos were electroporated *in ovo* with the indicated constructs as described in experimental procedures. Successfully electroporated embryos were harvested, bathed in medium and immediately imaged using confocal microscopy. Migrating neural crest cells were identified by their position and morphology. Green arrowheads indicate the presence of cWNT1-moxGFP in cellular projections while red arrowheads show the presence of WLS-mCherry in cellular projections. Images shown are representative of 121 different images taken on 12 different days.

overexpression of PORCN-mCherry had no overt effect on WNT1-moxGFP distribution, co-expression of WLS-mCherry had a pronounced effect. In the presence of overexpressed WLS-mCherry, we often observed that in addition to the expected localization in the ER and Golgi, WNT1-moxGFP was localized to the cell surface and to small cellular projections. Notably, this redistribution did not occur in all cells, but in a subpopulation of the cells that expressed both cWNT1-moxGFP and cWLS-mCherry. In sum, co-expression of WLS-mCherry, but not PORCN-mCherry, caused a redistribution of WNT1-moxGFP to the cell surface and to cellular projections.

3.7. WLS-mCherry, but not PORCN-mCherry, causes a redistribution of WNT1-moxGFP in chick neural crest and surface ectoderm cells

Lastly, we sought to determine the utility of these constructs in live chick embryos. To this end, we carried out live imaging of chick neural crest cells and surface ectoderm cells. In contrast to our observations in COS7 cells, we found that mCherry-tagged fusions, especially WLS-mCherry, were susceptible to aggregation (data not shown). Similar to our observations in COS7 cells (Figs. 5–6), cWNT1-moxGFP (Figs. 7 and 8, G-I) and PORCN-mCherry (Figs. 7 and 8, A-C) appeared in a pattern that is most closely resembles the endoplasmic reticulum. WLS-mCherry was observed in numerous punctae and on the cell surface (Figs. 7 and 8, D-F). In the neural crest cells, WLS was also localized to cellular projections (Fig. 7D). Whereas co-expression of mPORCN-mCherry along with cWNT1-moxGFP had no overt effect on the distribution of WNT1 in neural crest or ectodermal cells (Figs. 7 and 8, J-L), co-expression of WLS caused a redistribution of cWNT1-moxGFP to the surface of a subpopulation of cells expressing both cWNT1-moxGFP and WLS-mCherry (Figs. 7 and 8, M-O). In the neural crest cells, co-expression of WLS-mCherry also caused cWNT1-moxGFP to redistribute into cellular projections (Fig. 7M-O). Thus, co-expression of WLS-mCherry along with cWNT1-moxGFP stimulates a redistribution of WNT1 protein from the endomembrane system to the cell surface and cellular projections. We do not yet know if the recruitment of cWNT1-moxGFP into filopodia is specific or a byproduct of membrane localization.

4. Discussion

We have successfully developed a toolbox that facilitates the study of WNT1 palmitoylation and trafficking in cultured cells and tissues.

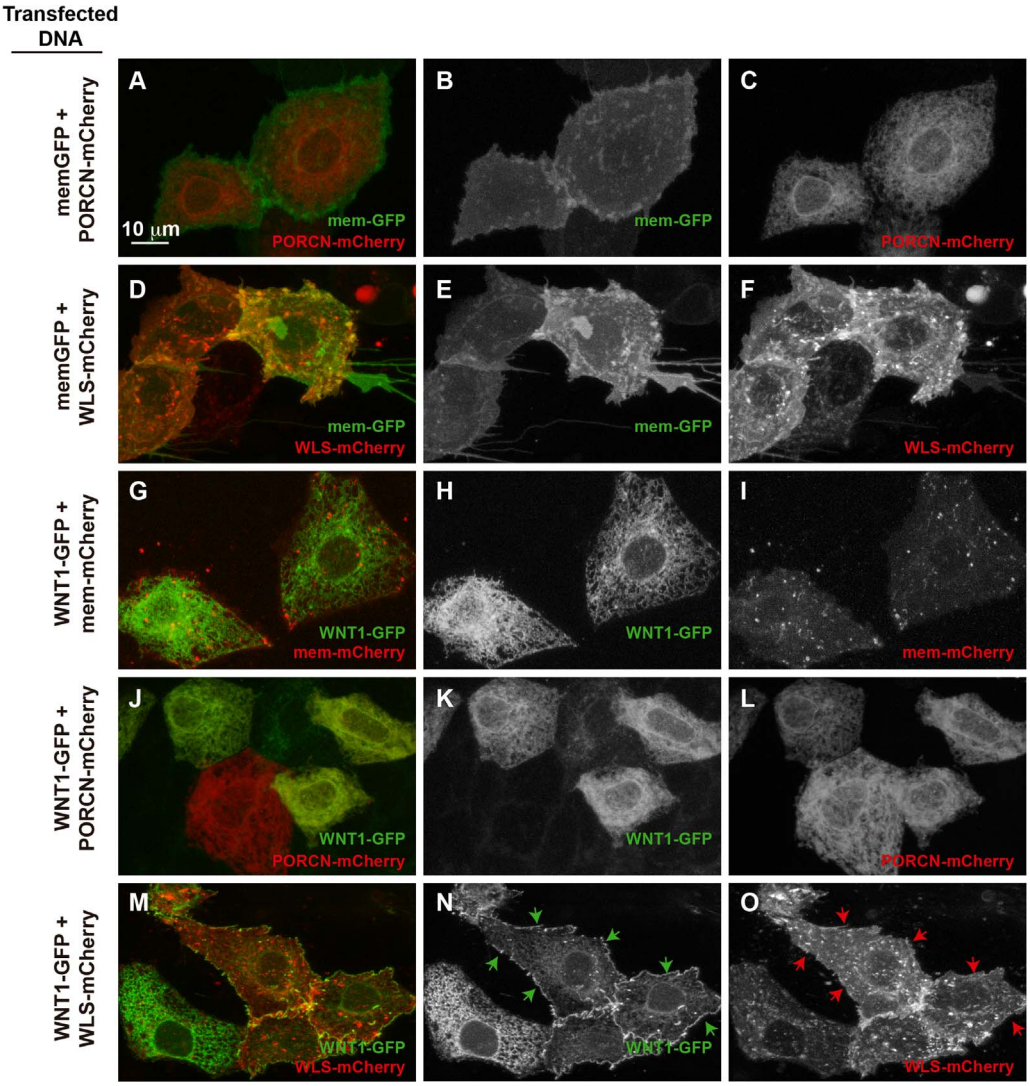

Fig. 8. Co-expression of WLS-mCherry, but not PORCN-mCherry, causes a redistribution of cWNT1-moxGFP from the endoplasmic reticulum to the plasma membrane in the surface ectoderm. Chick embryos were electroporated *in ovo* with the indicated constructs as described in experimental procedures. After a 24 h incubation, successfully electroporated embryos were harvested, bathed in medium and immediately imaged using confocal microscopy. Surface ectoderm cells were identified by their position and morphology. Green and red arrowheads indicate the localization of cWNT1-moxGFP and WLS-mCherry, respectively, to the cell surface. Images shown are representative of 44 many images taken on 6 different days.

Specifically, we have generated tagged variants of WNT1 that are useful for detecting palmitoylation using a click chemistry assay (cWNT1-Fc) and visualizing trafficking in live imaging experiments (cWNT1-moxGFP). The utility of these WNT1 fusions is enhanced by the development of biologically active mCherry-tagged PORCN and WLS variants. By expressing these constructs alone and in tandem, we are able to gain new insights about WNT1 palmitoylation and trafficking.

4.1. WNT1, but not WNT3A or WNT7A, is amenable to C-terminal tagging

Our studies clearly show that WNT1 from chick and zebrafish can tolerate C-terminal GFP and Fc tags. However, similarly tagged variants of cWNT3A and mWNT7A show activity that is only slightly above baseline. We further show that the number of linkers makes no difference with respect to biological activity. Our data combined with that of other labs shows that 3 Wnts, WNT1 (chick and zebrafish), WNT2B (Xenopus), and WNT8A (zebrafish), can be GFP-tagged on the C-terminus while numerous others cannot (Holzer et al., 2012; Luz et al., 2014; Stanganello et al., 2015). Although WNT3A is functionally similar to WNT1, our data along with that of Holzer and colleagues show that chick and mouse WNT3A are inactive upon tagging with GFP (Holzer et al., 2012). The subtleties of Wnt tagging are further highlighted by the observation that Xenopus WNT8-eGFP was inactive in one study while zebrafish WNT8A was active in others (Holzer et al., 2012; Luz et al., 2014; Stanganello et al., 2015).

4.2. WNT1-moxGFP outperforms WNT1-eGFP and WNT1-mCherry

We evaluated the activity and stability of fusion proteins with a variety of fluorophores. A number of years ago, a significant effort was made to generate a collection of Wnt constructs tagged with a C-terminal V5 epitope (Najdi et al., 2012). Unfortunately, these fusion proteins were well over 500 fold less active than their untagged counterparts. Subsequent studies by MacDonald and colleagues showed that the cysteine residue in V5 tagged Wnts formed inappropriate intramolecular disulfide bonds that were deleterious to activity (MacDonald et al., 2014). Substitution of the cysteine residue with a glycine restored secretion and activity to WNT3A. Thus, we predicted that cWNT1 fusions with the cysteine-less moxGFP would be significantly more active that those with eGFP. To our surprise, this was not the case. Thus, the cysteines in eGFP are apparently not

problematic for the secondary folding of WNT1. However, consistent with studies from the Snapp lab, our data show that the cWNT1-moxGFP fusion was significantly brighter than cWNT1-eGFP (Costantini et al., 2015). Though the moxGFP fusion was slightly less stable, the significant increase in fluorescent intensity was worth the small price in stability. cWNT1-mCherry also retained biological activity; however, it was considerably less bright than the moxGFP and exhibited significant degradation. Thus, cWNT1-moxGFP is our Wnt fusion of choice.

4.3. PORCN-mCherry and WLS-mCherry fusions add important tools to our emerging toolkit

Because of the success we had with cWNT1-moxGFP and zWnt1-eGFP, we chose to tag PORCN and WLS with mCherry so that we could simultaneously detect them along with WNT1-moxGFP. Both PORCN and WLS retained biological activity when tagged with mCherry and both yielded nice imaging results when introduced into cultured cells. When overexpressed in chick embryos, however, our mCherry tagged fusions showed significant aggregation. As this aggregation was particularly problematic for the WLS fusion, we think is likely that the existence of higher order WLS mulitmers is a contributing factor. To try and address aggregation issues associated with mCherry, we also generated WLS fusions with eGFP and mKate2. Alas, neither of these fusion proteins retained biological activity. Thus, we are still working to optimize the use of our mCherry fusions by reducing the levels of overexpression as well as the amount of time after transfection.

4.4. WLS levels are rate limiting in WNT1 trafficking

In numerous studies, overexpressed Wnt proteins have been primarily localized to the endoplasmic reticulum. Consistent with these data, cWNT1-moxGFP was primarily detected in the endoplasmic reticulum and the endomembrane system when overexpressed alone. Upon co-expression of WLS-mCherry, but not PORCN, cWNT1-moxGFP was redistributed to the plasma membrane and cellular projections. To our knowledge, these data represent the first direct visualization of WNT1 on the cell surface and in filopodia. Importantly, our images offer up an explanation for previously published work showing that co-expression of WLS, but not PORCN, promoted WNT1 signaling in a paracrine assay (Galli et al., 2016b). Our previous work also showed that the levels of WNT1 on the entire cell surface did not correlate well with activity (Galli et al., 2016b). Our detection of cWNT1-moxGFP in cellular projections (likely filopodia) is consistent with the notion that the localization of WNT1 to filopodia could be correlated with signaling. We are currently testing this prediction. Our results further agree with those of Proffitt and Virshup (2012) who showed that the levels of PORCN needed for full Wnt activity are extremely low.

Though the expression of WLS-mCherry along with cWNT1-moxGFP undoubtedly promoted the trafficking of WNT1 to the surface, the effects were somewhat variable. While cWNT1-moxGFP was clearly on the surface of some cells, it was not apparent on the cell surface of other cells. We have two hypotheses to explain these differences. First, because we carried out transient transfections, the relative amounts of WLS-mCherry and cWNT1-moxGFP vary from cell to cell. We have previously shown that the ratio of WLS to WNT1 is an important determinant of whether WLS promotes or inhibits Wnt signaling (Galli et al., 2014). A second possibility is that even in the presence of WLS, WNT1 is only found at the cell surface during particular phases of the cell cycle. We are currently testing these two models.

In conclusion, the tools that we have developed allow for detection of WNT1 palmitoylation in biochemical assays and localization of WNT1 in living cells and tissues. Co-expression of WLS-mCherry allows for the first direct visualization of vertebrate WNT1 on the cell surface and in cellular projections. Our experiments further provide a visual demonstration of the important, and rate limiting, role of WLS in the trafficking of WNT1 to the cell surface.

Acknowledgements

We thank Dr. Annette Chan of the Cell and Molecular Imaging Center for her assistance with confocal microscopy (SFSU). This research was made possible by NSF RUI IOS 0950892, NSF RUI MCB 1244602 and CSUPERB Grants to Dr. Laura Burrus and a NIH-RIMI (P20MD000262) Grant to San Francisco State University. Frederick Santana was supported by an NIH MARC fellowship (T34-GM008574) while Keri Ngo was supported by an NSF REU fellowship (DBI-1156452).

References

Bänziger, C., Soldini, D., Schutt, C., Zipperlen, P., Hausmann, G., Basler, K., 2006. Wntless, a conserved membrane protein dedicated to the secretion of Wnt proteins from signaling cells. Cell 125, 509–522.

Barrott, J.J., Cash, G.M., Smith, A.P., Barrow, J.R., Murtaugh, L.C., 2011. Deletion of mouse Porcn blocks Wnt ligand secretion and reveals an ectodermal etiology of human focal dermal hypoplasia/Goltz syndrome. Proc. Natl. Acad. Sci. USA 108, 12752–12757.

Bartscherer, K., Pelte, N., Ingelfinger, D., Boutros, M., 2006. Secretion of Wnt ligands requires Evi, a conserved transmembrane protein. Cell 125, 523–533.

Biechele, S., Cox, B.J., Rossant, J., 2011. Porcupine homolog is required for canonical Wnt signaling and gastrulation in mouse embryos. Dev. Biol..

Brown, A.M., Papkoff, J., Fung, Y.K., Shackleford, G.M., Varmus, H.E., 1987. Identification of protein products encoded by the proto-oncogene int-1. Mol. Cell. Biol. 7, 3971–3977.

Burrus, L.W., McMahon, A.P., 1995. Biochemical analysis of murine Wnt proteins reveals both shared and distinct properties. Exp. Cell Res. 220, 363–373.

Chen, B., Dodge, M.E., Tang, W., Lu, J., Ma, Z., Fan, C.W., Wei, S., Hao, W., Kilgore, J., Williams, N.S., Roth, M.G., Amatruda, J.F., Chen, C., Lum, L., 2009. Small molecule-mediated disruption of Wnt-dependent signaling in tissue regeneration and cancer. Nat. Chem. Biol. 5, 100–107.

Chen, X., Zaro, J., Shen, W.C., 2013. Fusion protein linkers: property, design and functionality. Adv. Drug Deliv. Rev. 65, 1357–1369.

Coombs, G.S., Yu, J., Canning, C.A., Veltri, C.A., Covey, T.M., Cheong, J.K., Utomo, V., Banerjee, N., Zhang, Z.H., Jadulco, R.C., Concepcion, G.P., Bugni, T.S., Harper, M.K., Mihalek, I., Jones, C.M., Ireland, C.M., Virshup, D.M., 2010. WLS-dependent secretion of WNT3A requires Ser209 acylation and vacuolar acidification. J. Cell Sci. 123, 3357–3367.

Costantini, L.M., Baloban, M., Markwardt, M.L., Rizzo, M., Guo, F., Verkhusha, V.V., Snapp, E.L., 2015. A palette of fluorescent proteins optimized for diverse cellular environments. Nat. Commun. 6, 7670.

Doubravska, L., Krausova, M., Gradl, D., Vojtechova, M., Tumova, L., Lukas, J., Valenta, T., Pospichalova, V., Fafilek, B., Plachy, J., Sebesta, O., Korinek, V., 2011. Fatty acid modification of WNT1 and WNT3a at serine is prerequisite for lipidation at cysteine and is essential for WNT signalling. Cell Signal 23, 837–848.

Farin, H.F., Jordens, I., Mosa, M.H., Basak, O., Korving, J., Tauriello, D.V., de Punder, K., Angers, S., Peters, P.J., Maurice, M.M., Clevers, H., 2016. Visualization of a short-range Wnt gradient in the intestinal stem-cell niche. Nature 530, 340–343.

Fu, J., Jiang, M., Mirando, A.J., Yu, H.M., Hsu, W., 2009. Reciprocal regulation of Wnt and Gpr177/mouse Wntless is required for embryonic axis formation. Proc. Natl. Acad. Sci. USA 106, 18598–18603.

Galli, L.M., Barnes, T., Burrus, L.W., 2016a. The use of chick embryos to study Wnt activity gradients. Methods Mol. Biol. 1481, 69–80.

Galli, L.M., Barnes, T.L., Secrest, S.S., Kadowaki, T., Burrus, L.W., 2007. Porcupine-mediated lipid-modification regulates the activity and distribution of Wnt proteins in the chick neural tube. Development 134, 3339–3348.

Galli, L.M., Burrus, L.W., 2011. Differential palmit(e)oylation of Wnt1 on C93 and S224 residues has overlapping and distinct consequences. PLoS One 6, e26636.

Galli, L.M., Szabo, L.A., Li, L., Htaik, Y.M., Onguka, O., Burrus, L.W., 2014. Concentration-dependent effects of WNTLESS on WNT1/3A signaling. Dev. Dyn..

Galli, L.M., Zebarjadi, N., Li, L., Lingappa, V.R., Burrus, L.W., 2016b. Divergent effects of Porcupine and Wntless on WNT1 trafficking, secretion, and signaling. Exp. Cell Res. 347, 171–183.

Gao, X., Arenas-Ramirez, N., Scales, S.J., Hannoush, R.N., 2011. Membrane targeting of palmitoylated Wnt and Hedgehog revealed by chemical probes. FEBS Lett. 585, 2501–2506.

Gao, X., Hannoush, R.N., 2014a. Method for cellular imaging of palmitoylated proteins with clickable probes and proximity ligation applied to Hedgehog, tubulin, and Ras. J. Am. Chem. Soc. 136, 4544–4550.

Gao, X., Hannoush, R.N., 2014b. Single-cell imaging of Wnt palmitoylation by the acyltransferase porcupine. Nat. Chem. Biol. 10, 61–68.

Goodman, R.M., Thombre, S., Firtina, Z., Gray, D., Betts, D., Roebuck, J., Spana, E.P., Selva, E.M., 2006. Sprinter: a novel transmembrane protein required for Wg secretion and signaling. Development 133, 4901–4911.

Gross, J.C., Chaudhary, V., Bartscherer, K., Boutros, M., 2012. Active Wnt proteins are secreted on exosomes. Nat. Cell Biol. 14, 1036–1045.

Hamburger, V., Hamilton, H.L., 1951. A series of normal stages in the development of the chick embryo. J. Morphol. 88, 49–92.
Hannoush, R.N., Arenas-Ramirez, N., 2009. Imaging the lipidome:omega-alkynyl fatty acids for detection and cellular visualization of lipid-modified proteins. ACS Chem. Biol. 4, 581–587.
Hannoush, R.N., Sun, J., 2010. The chemical toolbox for monitoring protein fatty acylation and prenylation. Nat. Chem. Biol. 6, 498–506.
Herr, P., Basler, K., 2012. Porcupine-mediated lipidation is required for Wnt recognition by Wls. Dev. Biol. 361, 392–402.
Holzer, T., Liffers, K., Rahm, K., Trageser, B., Ozbek, S., Gradl, D., 2012. Live imaging of active fluorophore labelled Wnt proteins. FEBS Lett. 586, 1638–1644.
Huang, H., Kornberg, T.B., 2015. Myoblast cytonemes mediate Wg signaling from the wing imaginal disc and Delta-Notch signaling to the air sac primordium. eLife 4, e06114.
Komekado, H., Yamamoto, H., Chiba, T., Kikuchi, A., 2007. Glycosylation and palmitoylation of Wnt-3a are coupled to produce an active form of Wnt-3a. Genes Cells 12, 521–534.
Kurayoshi, M., Yamamoto, H., Izumi, S., Kikuchi, A., 2007. Post-translational palmitoylation and glycosylation of Wnt-5a are necessary for its signalling. Biochem. J. 402, 515–523.
Luz, M., Spannl-Muller, S., Ozhan, G., Kagermeier-Schenk, B., Rhinn, M., Weidinger, G., Brand, M., 2014. Dynamic association with donor cell filopodia and lipid-modification are essential features of Wnt8a during patterning of the zebrafish neuroectoderm. PLoS One 9, e84922.
MacDonald, B.T., Hien, A., Zhang, X., Iranloye, O., Virshup, D.M., Waterman, M.L., He, X., 2014. Disulfide bond requirements for active Wnt ligands. J. Biol. Chem. 289, 18122–18136.
Megason, S.G., McMahon, A.P., 2002. A mitogen gradient of dorsal midline Wnts organizes growth in the CNS. Development 129, 2087–2098.
Mikels, A.J., Nusse, R., 2006a. Purified Wnt5a protein activates or inhibits beta-catenin-TCF signaling depending on receptor context. PLoS Biol. 4, e115.
Mikels, A.J., Nusse, R., 2006b. Wnts as ligands: processing, secretion and reception. Oncogene 25, 7461–7468.
Miranda, M., Galli, L.M., Enriquez, M., Szabo, L.A., Gao, X., Hannoush, R.N., Burrus, L.W., 2014. Identification of the WNT1 residues required for palmitoylation by Porcupine. FEBS Lett. 588, 4815–4824.
Najdi, R., Proffitt, K., Sprowl, S., Kaur, S., Yu, J., Covey, T.M., Virshup, D.M., Waterman, M.L., 2012. A uniform human Wnt expression library reveals a shared secretory pathway and unique signaling activities. Differ. Res. Biol. Divers. 84, 203–213.
Neumann, S., Coudreuse, D.Y., van der Westhuyzen, D.R., Eckhardt, E.R., Korswagen, H.C., Schmitz, G., Sprong, H., 2009. Mammalian Wnt3a is released on lipoprotein particles. Traffic 10, 334–343.
Papkoff, J., Brown, A.M., Varmus, H.E., 1987. The int-1 proto-oncogene products are glycoproteins that appear to enter the secretory pathway. Mol. Cell. Biol. 7, 3978–3984.
Petko, J., Tranchina, T., Patel, G., Levenson, R., Justice-Bitner, S., 2017. Identifying novel members of the Wntless interactome through genetic and candidate gene approaches. Brain Res. Bull..
Proffitt, K.D., Virshup, D.M., 2012. Precise regulation of porcupine activity is required for physiological Wnt signaling. J. Biol. Chem. 287, 34167–34178.
Ramirez-Weber, F.A., Kornberg, T.B., 1999. Cytonemes: cellular processes that project to the principal signaling center in Drosophila imaginal discs. Cell 97, 599–607.
Shcherbo, D., Murphy, C.S., Ermakova, G.V., Solovieva, E.A., Chepurnykh, T.V., Shcheglov, A.S., Verkhusha, V.V., Pletnev, V.Z., Hazelwood, K.L., Roche, P.M., Lukyanov, S., Zaraisky, A.G., Davidson, M.W., Chudakov, D.M., 2009. Far-red fluorescent tags for protein imaging in living tissues. Biochem. J. 418, 567–574.
Shibamoto, S., Higano, K., Takada, R., Ito, F., Takeichi, M., Takada, S., 1998. Cytoskeletal reorganization by soluble Wnt-3a protein signalling. Genes Cells 3, 659–670.
Smolich, B.D., McMahon, J.A., McMahon, A.P., Papkoff, J., 1993. Wnt family proteins are secreted and associated with the cell surface. Mol. Biol. Cell 4, 1267–1275.
Stanganello, E., Hagemann, A.I., Mattes, B., Sinner, C., Meyen, D., Weber, S., Schug, A., Raz, E., Scholpp, S., 2015. Filopodia-based Wnt transport during vertebrate tissue patterning. Nat. Commun. 6, 5846.
Takada, R., Satomi, Y., Kurata, T., Ueno, N., Norioka, S., Kondoh, H., Takao, T., Takada, S., 2006. Monounsaturated fatty acid modification of Wnt protein: its role in Wnt secretion. Dev. Cell 11, 791–801.
van den Heuvel, M., Harryman-Samos, C., Klingensmith, J., Perrimon, N., Nusse, R., 1993. Mutations in the segment polarity genes wingless and porcupine impair secretion of the wingless protein. EMBO J. 12, 5293–5302.
Veeman, M.T., Axelrod, J.D., Moon, R.T., 2003. A second canon. Functions and mechanisms of beta-catenin-independent Wnt signaling. Dev. Cell 5, 367–377.
Willert, K., Brown, J.D., Danenberg, E., Duncan, A.W., Weissman, I.L., Reya, T., Yates, J.R., 3rd, Nusse, R., 2003. Wnt proteins are lipid-modified and can act as stem cell growth factors. Nature 423, 448–452.